Accepted Manuscript

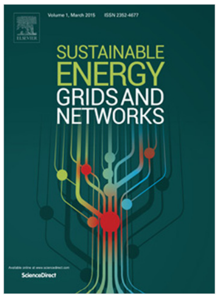

Improved -salp swarm optimized type-II fuzzy controller in load frequency control of multi area islanded AC microgrid

Prakash Chandra Sahu, Sonalika Mishra, Ramesh Chandra Prusty, Sidhartha Panda

PII: S2352-4677(18)30336-9
DOI: https://doi.org/10.1016/j.segan.2018.10.003
Reference: SEGAN 173

To appear in: *Sustainable Energy, Grids and Networks*

Received date : 11 September 2018
Revised date : 16 October 2018
Accepted date : 28 October 2018

Please cite this article as:, Improved -salp swarm optimized type-II fuzzy controller in load frequency control of multi area islanded AC microgrid, *Sustainable Energy, Grids and Networks* (2018), https://doi.org/10.1016/j.segan.2018.10.003

Improved -Salp Swarm Optimized type-II fuzzy controller in Load Frequency Control of multi area Islanded AC Microgrid.

Prakash Chandra Sahu, Sonalika Mishra, Ramesh Chandra Prusty Sidhartha Panda
Department of Electrical Engineering, VSSUT, Burla, 768018,Odisha, India
[a]prakashsahu.iter@gmail.com[c]ramesh.prusty82@gmail.com,[d]sidhartha_panda@rediffmail.com

Abstract

The present article deals with load frequency control (LFC) in an islanded two area AC microgrid (MC) system. In this study the proposed two area MG system comprises different micro sources including Micro-turbine (MT), Diesel engine generator (DEG) and Fuel Cells (FC) which are primarily responsible for balancing load and power generation in an interconnected system. MG in grid-connected mode has lower possibility of frequency control problem due to active presence of utility grid. Whereas MG in islanded mode faces huge frequency control problem due to dynamic nature of different renewable energy sources (RES) and different uncertainties like wind power fluctuation, disturbances in solar irradiation power, dynamics in applied load and system parameters (damping coefficient & Inertia constant). In regard to this the present article proposes a robust type-II fuzzy PID controller to create secondary frequency control loop for maintaining both frequency and tie-line power to their nominal values under different uncertainties. For performance study, the proposed type-II fuzzy PID controller performances are compared with type-I fuzzy controller, PID and PI controllers. To obtain optimal gain values of above controllers, a meta-heuristic improved-salp swarm optimization (I-SSO) algorithm has been implemented and proposed I-SSO technique performances are compared with original SSO, Particle swarm optimization (PSO) and Genetic Algorithm (GA) techniques. Finally it is observed from different performance analysis that proposed I-SSO tuned type-II fuzzy controller exhibits superior performances for load frequency control in multi-area islanded AC microgrid system under different uncertainty conditions.

Keywords: *Load Frequency Control (LFC); Area Control Error (ACE); Distributed Generation (DG); Salp Swarm Optimization (SSO); Renewable Energy Sources (RES); Type-II Fuzzy PID Controller;*

1. Introduction

Microgrid is a small digital controlled grid, where large number of distributed generations (DG) are connected for providing electrical energy especially in remote and distant areas. In economical point of view, installation of utility grid in remote areas paves more costly and is not reliable due to far from different generating stations. In view of this to produce pollution free electrical energy with cost effective most of remote and distant areas are facilitated with microgrids [1-2] for fulfilling electrical demand of different consumers. In recent energy scenario, the advanced technology promotes to most of researchers for getting electrical energy from different renewable sources. So research has been carried out to generate electrical energy through wind energy source, solar irradiation power, tidal energy, geothermal energy etc. Besides this to provide electrical energy over small locality different micro sources like diesel engine generator (DEG), Micro turbine (MT) and Fuel Cells (FC) have been utilized successfully[3-6]. In this regard to consume power judiciously, different energy storing devices like Battery energy storage (BES), Ultra capacitor and Flywheel energy storage (FES) devices have been equipped in AC microgrid systems [7-8]. The different micro sources and storage devices inspire to develop microgrid system.

In operational point of view microgrids are operated with two basic modes i.e. Grid connected mode and Islanded (off-grid) mode [9-10]. Control mechanism in islanded mode is very difficult and creates huge challenges for power engineers than grid connected mode. Because in grid connected mode, deviations in voltage and frequency due to different uncertainties are compensated by active utility grid. In islanded mode, in some extent few energy sources are efficient to compensate load fluctuations and uncertainties in wind power and solar irradiation power, but for reliable operation and to maintain balance between generation and demand (LFC) [11-14] different control mechanisms are required for islanded AC micro grid system. In islanded micro grid system, the most challenging factors of distributed energy resources (DER) are uncertainties, low inertia, dynamic nature and non linear structure. Any of above factor can create mismatch between the generation and demand of the MG system which leads deviation in both frequency and tie-line power from their respective nominal values. To obtain robust performance of the MG system, improve control strategy is essential as powerful solution under different environmental and load conditions. While designing different distributed energy resources for an islanded MG system, some important factors like economic constraints and environmental conditions are taken in to consideration [15]. In view of this weather dependent DERs like wind energy resource and Photo Voltaic (PV) system will not be participated for secondary frequency and tie-line power control [16]. Weather independent resources like DEG, MT and FC are favored to supply energy for demand side to support net electrical energy of the system. Slower response times of above DERs make them inefficient to control the MG system quickly in response to sudden change of load. To improve compensation time period and controllability of MG system, different energy storage devices like Battery energy storage (BES) and Flywheel energy storage [FES] are required to coordinate with different resources of MG system [17-18].

It has been observed through different research articles that, alike conventional power system different hierarchical control approaches have been proposed for frequency and power control of islanded MG system. The objective of this article is to implement advanced control mechanism to create secondary frequency regulation loop of MG system. This secondary control loop tries to maintain both frequency and tie-line power of the system within their nominal values in order to keep system stable under any uncertainty conditions. MG system with secondary control loop employs two different MG structures i.e. Centralized structure and decentralized structure [19]. MG central controller (MGCC) operation is influenced by centralized structure and in decentralized structure; all equipped energy sources in MG system are well interacted with each other. In regard to this centralized structure is suitable for islanded MG system and decentralized structure is more suitable for grid-connected mode. The article aims to propose a centralized structure for both frequency and power control of MG system. To obtain robust MG system, different robust controllers have been proposed and are demonstrated through literatures [20-21]. In this regard to obtain secondary control loop, Bevrani et.al. proposed μ-synthesis approach in single area MG system [22]. In review of μ-synthesis, Kahrobaeian et.al.[23] has proposed μ-synthesis in some complex work. Rajendra et.al.[24] proposed multistage PID controller for frequency control in an islanded single are MG system The conventional PID controllers are less sensitive to different uncertainty conditions. In regard to this the present article proposes a robust type-II fuzzy PID controller for controlling both frequency and tie-line power of islanded MG system under different uncertainties (dynamics in ΔP_D, fluctuation in wind power ΔP_W, fluctuation in solar irradiation power ΔP_Φ) . From few decades, it has been creating challenges for researchers to obtain optimal gain values of different proposed controllers. In this regard Guerreo et.al. proposed hopfield fuzzy neural network technique and hybridized particle swarm optimization and fuzzy logic method [25] for frequency control in MG system. Rajendra et.al. [26] proposed novel dragonfly optimization and pattern search algorithm for frequency control in single area MG system. The present article proposes a maiden approach of novel improved-salp swarm optimization (I-SSO) technique for optimizing gain parameters of proposed type-II fuzzy PID controller.

1.1 Contribution

The aim of this article is to obtain load frequency control in an islanded two area microgrid system and is demonstrated briefly through different steps.

I. Different micro sources like DEG, MT, FC, PV and wind generator are assembled together to constitute a microgrid system.

II. To improve coordinating between generation and demand, energy storage devices like BES and FES are integrated with common MG system.

III. Under different uncertainties (ΔP_D, ΔP_W and ΔP_Φ) and dynamics in system parameter (M, H) a type-II fuzzy PID controller is proposed to create necessary MG control mechanism.

IV. Different gain parameters of proposed controller are optimized with novel I-SSO technique.

V. Finally to justify supremacy of proposed type-II fuzzy controller it's performances are compared with type-I fuzzy controller, conventional PID and PI controllers and in technique level the performances of proposed I-SSO technique is compared with original SSO, PSO and GA algorithms.

VI. In regard to load frequency control of islanded two area MG system, proposed I-SSO optimized type-II fuzzy controller exhibits superior performance over other implemented approaches.

2. System under study

A. Microgrid Model with LFC

A simplified transfer function model of two equal area AC microgrid system in islanded mode is depicted in Fig.1. Each area has an average capacity of 10MW and with average load of 6MW. Each area comprises different micro sources like DEG, MT, FC, PV and WTG along with few energy storage devices like BES and FES. In this simplified model individual micro sources and energy storage devices are demonstrated through their equivalent transfer function expressions. Fig.2 depicts detailed configuration of a single area MG system. The transfer function expression for individual system is as follows.

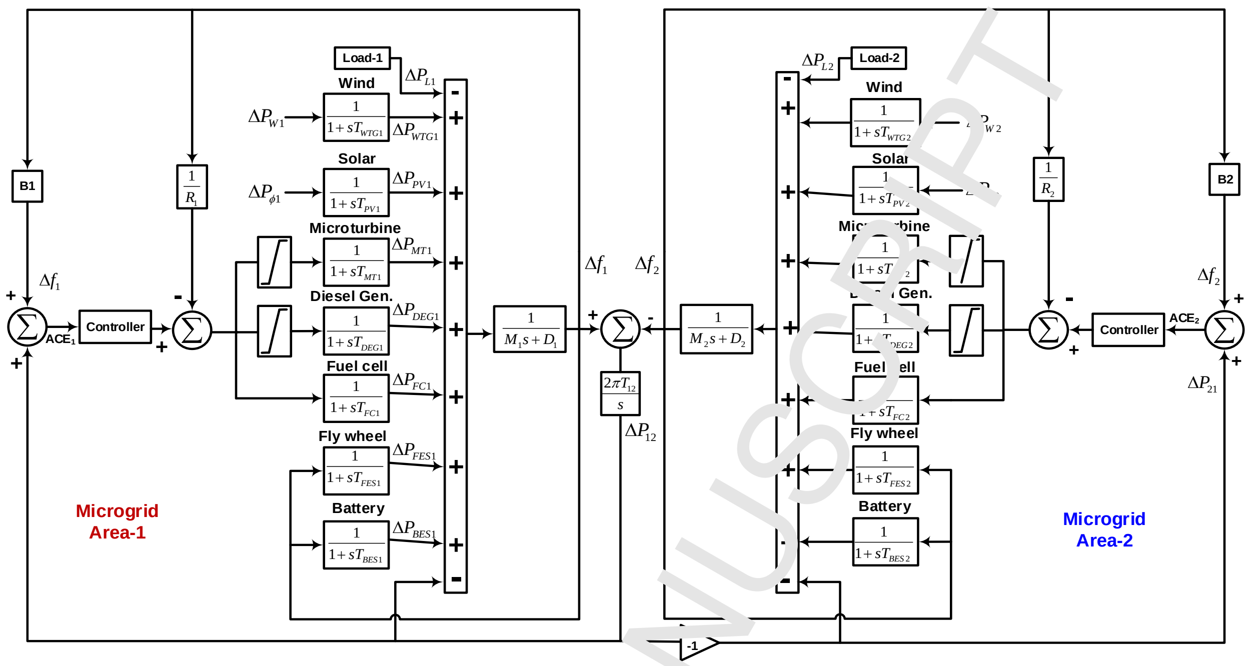

Fig.1 Two-area interconnected islanding Microgrid system under study.

I. Diesel Engine Generator (DEG)

$$G_{DEG}(s) = \frac{\Delta P_{DEG}(s)}{\Delta P_{DE}(s)} = \frac{1}{1+s.T_{DEG}} \tag{1}$$

ΔP_{DEG} = Output power deviation; ΔP_{DE} = Input power deviation; T_{DEG} = Time constant of diesel generator.

II. Micro turbine (MT).

$$G_{MT}(s) = \frac{\Delta P_{MT}(s)}{\Delta P_{M}(s)} = \frac{1}{1+s.T_{MT}} \tag{2}$$

ΔP_{MT} = Output power deviation; ΔP_{M} = Input power deviation; T_{MT} = Time constant of micro turbine.

III. Fuel Cells (FC)

$$G_{FC}(s) = \frac{\Delta P_{FC}(s)}{\Delta P_{F}(s)} = \frac{1}{1+s.T_{FC}} \tag{3}$$

ΔP_{FC} = Output power deviation; ΔP_{F} = Input power deviation; T_{FC} = Time constant of micro turbine.

IV. Wind turbine generator (WTG)

$$G_{WTG}(s) = \frac{\Delta P_{WTG}(s)}{\Delta P_{W}(s)} = \frac{1}{1+s.T_{WTG}} \tag{4}$$

ΔP_{WTG} = Output power deviation; ΔP_{W} = Input power deviation; T_{WTG} = Time constant of wind generator.

V. Photo Voltaic (PV)

$$G_{PV}(s) = \frac{\Delta P_{PV}(s)}{\Delta P_{P}(s)} = \frac{1}{1+s.T_{PV}} \tag{5}$$

ΔP_{PV} = Output power deviation; ΔP_{P} = Input power deviation; T_{PV} = Time constant of photo voltaic cell.

VI. Battery Energy Storage (BES)

$$G_{BES}(s)=\frac{\Delta P_{BES}(s)}{\Delta P_{BE}(s)}=\frac{1}{1+s.T_{BES}} \quad (6)$$

$\Delta P_{BES}=$ Output power deviation; ΔP_{BE} = input power deviation; T_{BES} = Time constant of *BES*.

VII. Fly wheel Energy Storage (FES).

$$G_{FES}(s)=\frac{\Delta P_{FES}(s)}{\Delta P_{FE}(s)}=\frac{1}{1+s.T_{FES}} \quad (7)$$

$\Delta P_{FES}=$ Output power deviation; ΔP_{FE} = input power deviation; T_{FES} = Time constant of *FES*.

The total power generation in each individual area of MG system is

$$P_{total}=P_{DEG}+P_{MT}+P_{FC}+P_{WTG}+P_{PV}\pm P_{BES}\pm P_{FES} \quad (8)$$

From the transfer function model, it is more clear that only DEG, MT and FC micro sources are participating for secondary frequency control of MG system where as remaining WTG and PV system are not participating for secondary frequency control due to their large environmental condition depending nature.

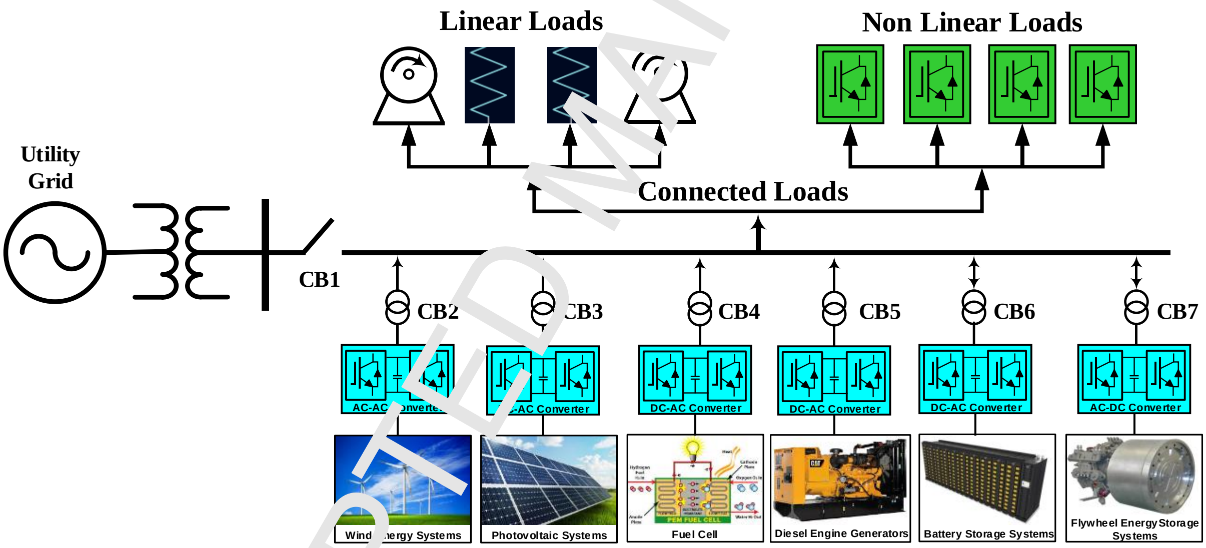

Fig.2 Configuration of an Islanded Microgrid System

3. Proposed Statement

3.1 Type-II Fuzzy PID Controller (type-II-FPID)

In type-I fuzzy controller the membership function exhibits a crisp value due to which a two dimensional presentation is incurred with this type of fuzzy system. Where as in type-II fuzzy system the related membership functions are created with the combination of both lower membership function (LMF) and upper membership function(UMF) of type-I fuzzy system. At foot prints of uncertainty (FOU) a barrier is created [27-28] due to the combination of both LMF and UPF and is depicted in Fig.4. FOU is the collective values of some primary membership function and is sandwiched between the interval of both LMF and UPF. The membership function of type-II fuzzy system holds 3D structure with enhanced degree of freedom. This advanced structure gracefully improves the uncertainties in LFC of electrical system. A fuzzy action is also occurred between the grades of type-II membership functions due to which it is able to enhance the fuzziness and simultaneously imprecise data and is controlled in a precise manner. Fig.5 depicts the entire process incurred with type-II fuzzy system. The detailed block diagram model of type-II fuzzy PID controller with corresponding operations is depicted in fig .6. The model of type-II fuzzy PID controller along with their scaling factors (K_1 and K_2) with derivative filter is depicted in Fig.3. To describe details of type-II fuzzy controller along with fuzzification and defuzzification [29] it goes through different steps.

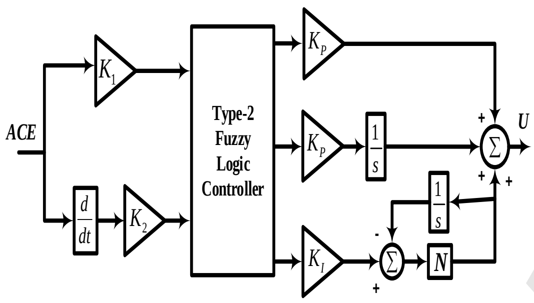

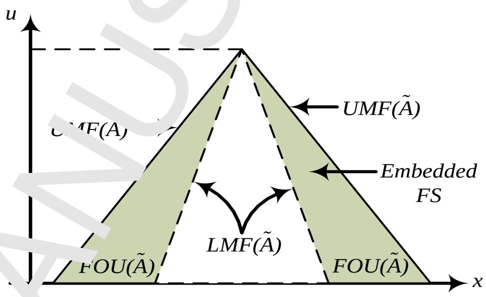

Fig.3.Type-II fuzzy controller with derivative filter **Fig.4** Structure of type-II fuzzy membership function with FOU

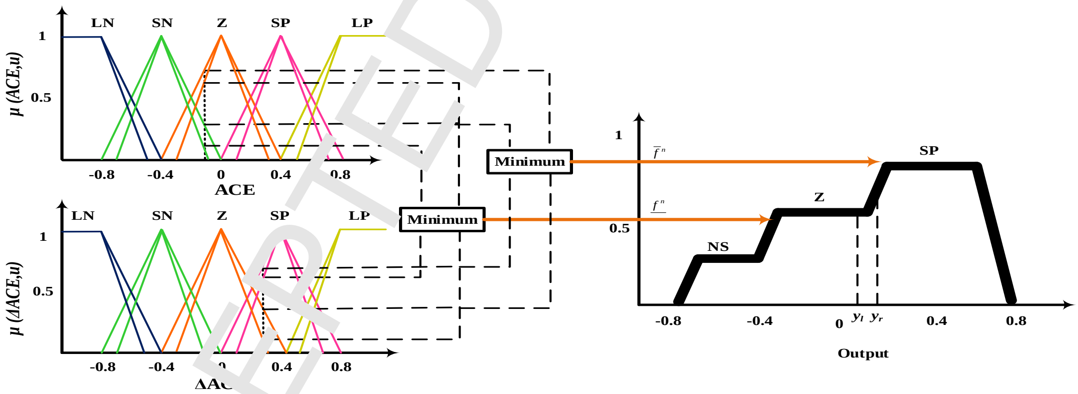

Fig.5 Membership functions with fuzzification and defuzzification process in type-II fuzzy controller.

<u>Fuzzifier</u>

Unlike type-I fuzzy controller the ACE and derivative of ACE (*dACE*) are referred as input variables for type-II fuzzy controller. The functions of fuzzifier it to convert these input variables to a 3D representation type-II fuzzy sets and finally it triggers to both inference and rule base.

Let E = type-II fuzzy set

μ_E (ACE,x)= Membership function

Mathematical representation of above set E is

E = ((ACE, x), μ_E (ACE, x)) |∀ACE € P, ∀x € J_{ACE} [0, 1]

In continuous universe of discourse , E may be equated as

$$E = \int_{ACE \in P} \int_{x \in J_{ACE}[0,1]} \frac{\mu_E(ACE, x)}{(ACE, x)} \quad [9]$$

Here ACE = Primary variable with domain P

X = Secondary variable with domain J_{ACE}

∫∫ = Union over ACE and x.

Both membership functions UMF $\mu_{\bar{E}}$ (ACE, x) and LMF $\mu_{\underline{E}}$ (ACE, x) are demonstrated through equation (10)

$$\mu_{\bar{E}}(ACE, x) = \overline{FOU(E)} \quad \forall ACE \in P, \forall x \in J_{ACE}[0,1] \quad [10]$$

J_{ACE} may be expressed as

$$J_{ACE} = [\mu_{\bar{E}}(ACE, x), \mu_{\underline{E}}(ACE, x)] \quad \forall ACE \in P, \forall x \in J_{ACE}[0,1] \quad [11]$$

All membership functions of type-I fuzzy controller help to build UMFs of type-II fuzzy system and to create LMFs the points of UMFs are shifted with zero membership function grades like ($\overline{ACE_1}$) to $\underline{ACE_1}$ and UMFs ($\overline{ACE_2}$) to $\underline{ACE_2}$ and the detail is depicted in Fig.4. Unlike type-I fuzzy controller, different linguistic variables used for both input and output in type-II fuzzy controller are Negative high (NH), Negative low (NL), Zero (Z), Positive Low (PL) and Positive high (PH) and is demonstrated through table.1

Table.1 Rule base of type-II fuzzy system.

e \ $\dot{e}$	NH	NL	Z	PL	PH
NH	NH	NH	NL	Z	NL
NL	NH	NL	NL	PL	Z
Z	NL	NL	Z	PL	PL
PL	Z	PL	PL	PH	PH
PH	NL	Z	PL	PH	PL

Knowledge Base

Rule base and interface engine are two basic building block of knowledge base which are depicted details in Fig.6. Different linguistic variables such as Negative high (NH), Negative low (NL), Zero (Z), Positive Low (PL) and

Positive high (PH) are used in the rule base of type-II fuzzy system which are depicted in table.1. In type-II fuzzy system ACE and derivative of ACE (*dACE*) are referred as input signal and y is assumed to be output signal.

The property of type-II fuzzy system is expressed as

LMF : For ACE = <u>NS</u>; *dACE* = <u>Z ;</u> Output y = <u>NS</u> .

UMF : For ACE = $\overline{NS}$; *dACE* = $\overline{Z}$;Output y = $\overline{NS}$.

The type-II fuzzy set's firing strength may be expressed as

$$\underline{f^K} = \min(\mu_{\overline{EK}}(ACE, x), \mu_{\overline{EK}}(dACE, x)) .$$

$$\overline{f^K} = \max(\mu_{\overline{EK}}(ACE, x), \mu_{\overline{EK}}(dACE, x)) .$$

$$F^K = [\underline{f^K}, \overline{f^K}] \text{ , K = 1, 2 …25} \qquad .[12]$$

<u>Defuzzifier and type reducer</u>

The function of type reducer is to convert type-II fuzzy sets to type-I fuzzy set with smooth operation. Different methods associated for this fuzzy set conversion mechanism are center of sums, center of sets, height, centroid etc. It has been observed that center of sets (COS) method is most prominent method for reduction of fuzzy sets.

$$Y_{COS} = \sum_{K=1}^{25} \frac{F^K Y^K}{F^K} = [y_{m1}, y_{m2}] \qquad [13]$$

$$y_{m1} = \frac{\sum_{K=1}^{25} \underline{f^K}\,\underline{y^K}}{\sum_{K=1}^{25} \overline{f^K}}$$

$$y_{m2} = \frac{\sum_{K=1}^{25} \overline{f^K}\,\overline{y^K}}{\sum_{K=1}^{25} \overline{f^K}}$$

; [14]

Here y_{m1} = Solution to minimize problem; y_{m2} = Solution to maximize problem.

Both y_{m1} and y_{m2} are treated as two membership function of type-I fuzzy system and are derived from a single type-II membership function. The crisp output of fuzzy-II fuzzy system is obtained with averaging both y_{m1} and y_{m2} . To improve capability of proposed type-II fuzzy controller, the obtained crisp value is again passes through the proportional and integral controller. While designing proposed type-II fuzzy controller it has to be gone through different stages and also depicted in Fig.6

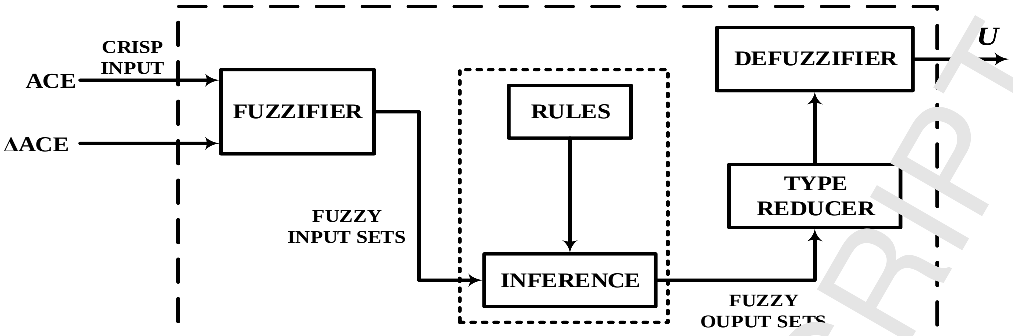

Fig.6 Block diagram of type-II fuzzy controller with different stages

3.2 Objective function

While optimizing different gain parameters of proposed controller it is required to choose most effective objective function such that it would produce dynamic responses having least overshoot, undershoot and settling time. In the area of optimization different objective function have been used i.e Integral of Time multiplied Absolute Error(ITAE), Time multiplied Squared Error(ITSE), Integral of Integral of Absolute Error(IAE) and Integral of Squared Error(ISE). The above objective functions follow certain constraints and execution conditions.. In this research article ITAE has been implemented as objective function due to its supremacy performance owing to least overshoot, undershoot and settling time based dynamic response producing capability.

ITAE is expressed through equation (15)

$$J=ITAE=\int_0^T \left(|\Delta F_i| + |\Delta P_{tiei-j}|\right) t\, dt \tag{15}$$

Where ΔF_i =frequency deviation i^{th}area, ΔP_{tiei-j}= tie line power deviation between $i^{th}$and j^{th}area and T = simulation time. The objective functions are minimized subject to the constraints given by $K_{P\,Min} \leq K_p \leq K_{P\,Max}$, $K_{D\,Min} \leq K_D \leq K_{D\,Max}$, $K_{I\,Min} \leq K_I \leq K_{I\,Max}$, $K_{1\,Min} \leq K_1 \leq K_{1\,Max}$,. Where range of all gains are [-2,2] .

4.1 Basic Salp Swarm Optimization(SSO) algorithm

Salp is one type of ocean creature which has transparent type barrel-shaped body structure and belongs to a family of salpidae. These species of organisms are very similar with jelly fish and also moves like jelly fish. The shape and structure of salp is shown in Fig7 (a). It is very tough to access the biological living environment of the salps. The swarming behaviour of salps is very funny and interesting. According to this at very deep oceans salp produces a swarm, known as salp chain and shown in Fig7 (b). Though the reason to produce such behaviour is not cleared but researchers believe this could be for achieving better locomotion. Though there is no definite mathematical model of salp swarm to solve optimization problems, the present research paper proposes maiden model of salp chains for solving different optimization problems [30]. While developing mathematical model, before that the population is splitted in two categories i.e leader and follower. In salp chain the leader remains at front of the chain to which other salps follow (follower). Similar to other type of swarm based optimization technique, the salp occupies a position and is defined in n-dimensional search space and n represents number of variables. There is a matrix 'X' which stores all the position of salps. In search space the main target of salp is food source and is represented by 'F'. The

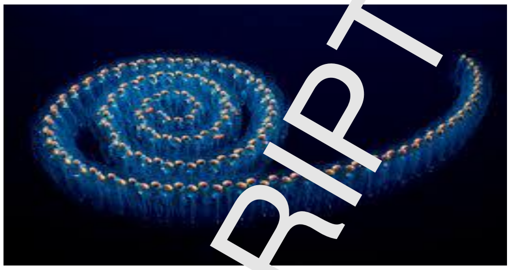

Fig.7 (a) single salp, (b) swarm of salp(salp chain)

below equation helps to update the position of leader.

$$X_j^1 = \begin{cases} F_j + C_1((ub_j - lb_j)C_2 + lb_j) & C_3 \geq 0 \\ F_J - C_1((ub_j - lb_j)C_2 + lb_j) & C_3 < 0 \end{cases} \tag{16}$$

Where X_j^1= position of leader in j^{th} dimension.; F_j = position of food source in j^{th} dimension

u_b & l_b = upper and lower bounds.; C_1, C_2& C_3 = random numbers. .

The random number C_1 helps to balance the exploration and exploitation and is equated as

$$C_1 = 2e^{-(\frac{4l}{L})^2} \tag{17}$$

Where l= current iteration; L=max number of iteration

Below equation helps to update the position of followers and is formed according to Newton's Law's of motion.

$$X_j^i = \frac{1}{2}at^2 + V_0 t \tag{18}$$

Where $i \geq 2$; X_j^i =Position of i^{th} follower salp in j^{th} dimension at time t sec; V_0 = initial speed

$$a = \frac{V_{finitial}}{V_0}; \text{ V= } \frac{x - x_0}{t} \tag{19}$$

Considering V_0 and discrepancy between iteration the modification of above equation will be

$$X_j^i = \frac{1}{2}(X_j^i + X_j^i - 1) \; i \geq 2 \tag{20}$$

Finally simulation of salp chain is occurred with the above equations.

4.2 Improved Salp Swarm Optimization (I-SSO) Algorithm

The original SSO algorithm though it solves different optimization problems efficiently but it is inefficient to solve multi-objective oriented problems due to following limitations.

I. To obtain best solution, SSO technique only stores one solution which is not sufficient for a multi-objective problem.

II. Though SSO technique updates each food source in response with best solution, but its single best solution obtaining ability is not suitable for multi-objective problems.

In order to solve different multi-objective problems, it is required to modify original SSO technique by updating different iterative equations and restructuring SSO technique with a repository of food destination [31]. During optimization the repository facility controls the best non-dominated solutions which are produced through this process. To save finite number of non-dominated solutions, the repository of food source is structured with maximum size. The pareto dominance operator [32-33] helps to compare each salp over all repository residents during optimization process. In case a salp leads from a solution in the repository they will be swapped accordingly but if a single salp leads over set of solutions in repository then all repository residents are replaced with the salp. In new population if a single repository resident dominates a salp, it must be discarded quickly. A salp will be added whenever it will be non-dominated in nature over all repository residents. A maximum distance with numbers of neighboring solutions is assumed while searching non-dominated solutions. The distance 'S' is expressed as $\vec{S} = \frac{\vec{\max} - \vec{\min}}{repositorysize}$. $\vec{\max}$ and $\vec{\min}$ are two vectors which stores maximum and minimum value of each solution respectively. In regards to number of neighboring solutions, each repository resident is assigned with suitable rank then best one is selected with the help of roulette wheel method.

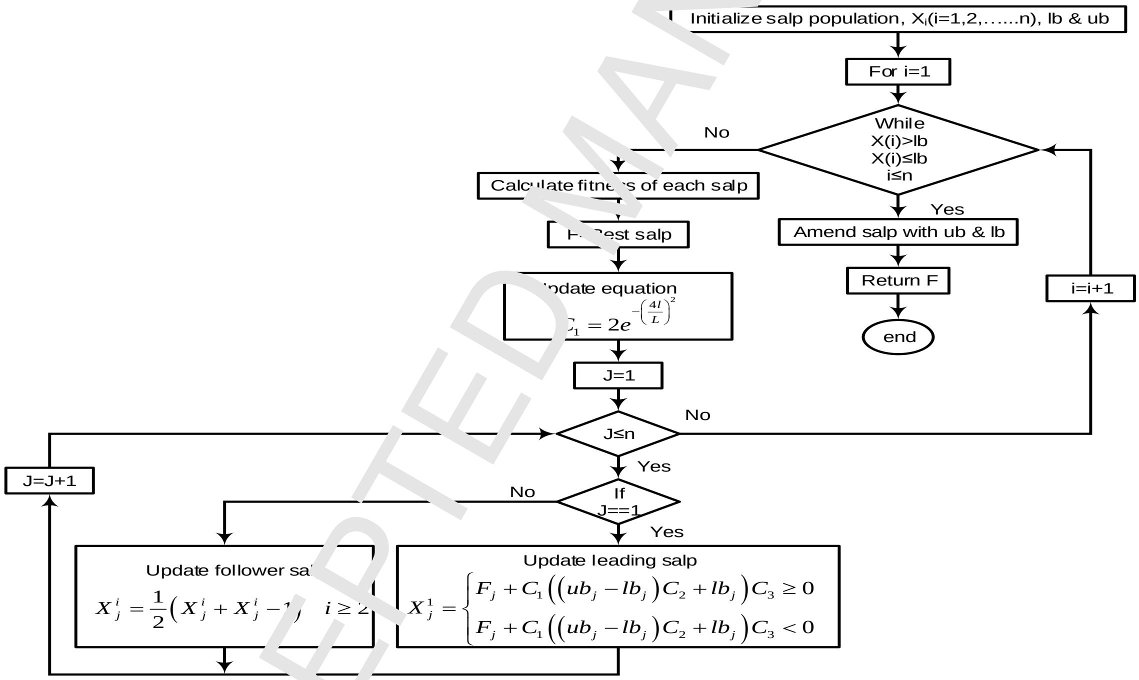

Fig. 8 Flow chart of I-SSO algorithm

The flow chart of proposed I-SSO algorithm is depicted in Fig.8. The I-SSO technique is followed through different steps.

Step.1:

Initialization of salp population with declaration of both upper bound and lower bound of variables.

Step.2:

Non-dominated salps are well defined after calculating objective value of each individual salp. In case the repository is empty all the non-dominated solutions are gathered in repository.

Step-3:

The repository is ready to delete the solution whenever the repository is full in assurance with neighborhood. The roulette wheel method helps to select the solution after ranking all the solutions.

Step-4

Non-dominated salps are gathered in repository after replacing lots of residents. Food source is marked from solutions after updating the repository by roulette wheel method.

Step-5

Random number C_1 is updated through equation (17) and equations (19) and (20) are utilized to update position of leader salp and follower salp respectively.

Step-6

Until to fetch satisfaction condition all the above steps are repeated except initialization (step-1)

5 Results and Analysis

This section deals with the presentation of different resulted dynamic responses i.e deviation in area frequency (Δf) and tie-line power (ΔP_{tie}) in response with various system uncertainties (ΔP_L, ΔP_W and ΔP_ϕ) with the presence of different optimized controllers. To obtain above response the two area transfer function model of interconnected MG system is developed in simulink environment and necessary programmes are written in .m file of MATLAB2016 software through 4GB ram *i*-5 processor based system. For load frequency control, the system uncertainties are effected individually and finally in combined form to trace out different dynamic responses. In this regard four different scenarios are considered for LFC study of two area interconnected MG system. *Scenario-1*: Variation of only load (ΔP_L), *Scenario-2*: Fluctuation of only wind power (ΔP_W), *Scenario-3*: Fluctuation of only solar irradiation power (ΔP_ϕ), *Scenario-4*: Combined fluctuation of all three uncertainties ($\Delta P_L + \Delta P_W + \Delta P_\phi$). For this study a type-II fuzzy PID controller is proposed for secondary frequency and tie-line power control of interconnected MG system and to obtain optimal gain values of proposed controller a meta-heuristic improved-salp swarm optimization (I-SSO) algorithm has been implemented. The viability of proposed type-II fuzzy controller is justified in comparison with performance with type-I fuzzy controller, conventional PID and PI controllers. The effectiveness of proposed I-SSO algorithm over original SSO, PSO and GA techniques is demonstrated through different comparative studies.

A. Controller Level

This study comprises different scenarios for LFC analysis in MG system along with different optimized controllers.

***Scenario-1*: Variation of only load (ΔP_L)**

In this case study to obtain LFC of an interconnected MG system a random pattern load (RLP) as shown in Fig.8(a) is effected in area1 at time t=0 while effected disturbances of wind and solar power is zero (ΔP_W=0, ΔP_ϕ=0). In regard to this disturbance, the deviated responses of frequency and tie-line power resulted due to different optimized controllers are depicted in this section. To obtain simulated dynamic responses, the optimal gain parameters in the range of [-2 2] of proposed type-II fuzzy PID controller due to I-SSO technique are gathered in table.2.The deviation in frequency of area1 and area2 due to I-SSO optimized type-II fuzzy PID, type-I fuzzy PID, PID and PID controllers are depicted in Fig.8(b-c) respectively. The tit-line power deviation is given in Fig.8 (d). Despite of their settling time, peak overshoot and peak undershoot, a significant improvement has been noticed in all dynamic responses resulted due to proposed I-SSO optimized type-II fuzzy PID controller. So our proposed approach exhibits more effectiveness over other implemented controllers for Load Frequency Control of MG system.

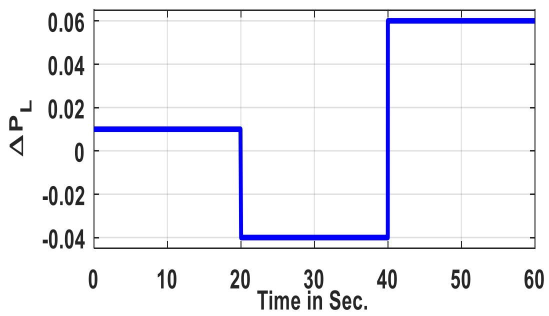

Fig. 8(a) Variation of load (**ΔP_L**)

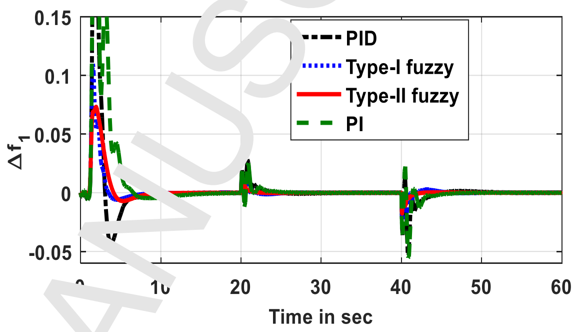

Fig. 8(b) Variation of area1 frequency due to **ΔP_L**

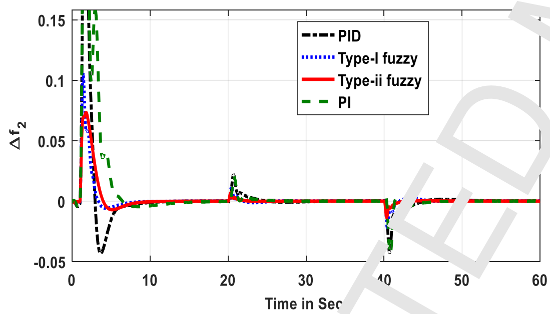

Fig. 8(c) Variation of area2 frequency due to **ΔP_L**

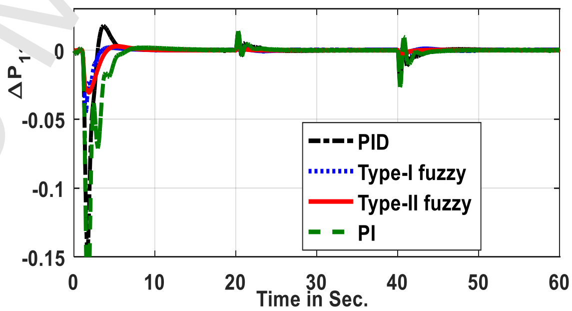

Fig. 8(d) Variation of tie-line power due to **ΔP_L**

Table.2 Optimal gain values of I-SSO optimized type-II fuzzy controller under different uncertainties

Area	Uncertainties	Type-II fuzzy PID Controller				
		K_P	K_I	K_D	K_1	K_2
Area.1	ΔP_L	-1.9516	-0.9692	-1.9922	-1.6252	0.0868
	ΔP_W	-1.9822	-1.7758	0.6898	0.8256	-1.2218
	ΔP_Φ	-1.6892	-1.9022	-1.1502	-1.6500	0.9868
	$\Delta P_L+\Delta P_W+\Delta P_\Phi$	-1.8964	-1.9696	-1.7786	-0.7862	1.2288
Area.2	ΔP_L	-0.8546	-1.9862	0.8707	-1.8686	-0.1582
	ΔP_W	-1.9688	-1.6562	-1.9900	0.7676	-1.4546
	ΔP_Φ	-0.7276	-1.9980	1.1456	-0.9802	0.5658
	$\Delta P_L+\Delta P_W+\Delta P_\Phi$	-0.8574	-1.8028	0.8968	0.2278	-0.4328

***Scenario-2*: Fluctuation in wind power only(ΔP_W), ΔP_L=0, ΔP_ϕ=0**

For this study a wind power fluctuation signal shown in Fig.9 (a) is effected at area1 at time t=0. All deviated responses due to different optimized controllers are depicted in Fig.9. In this regard Fig.9 (b-c) depicts deviation in responses of frequency of area1 and area2 respectively where as tie-line power deviation response is shown in Fig.9(d). Critical analysis on dynamic responses and table.3 reveals that I-SSO tuned type-II fuzzy PID controller exhibits superior performance over other implemented optimized controllers.

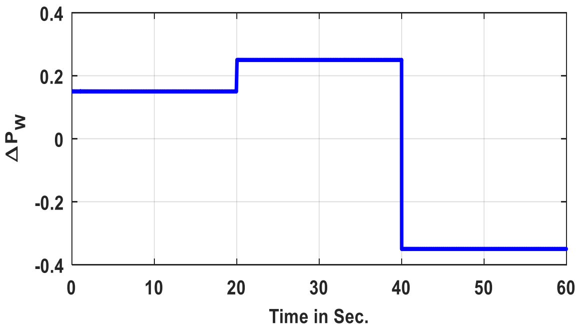

Fig. 9(a) Variation of wind power (ΔP_W)

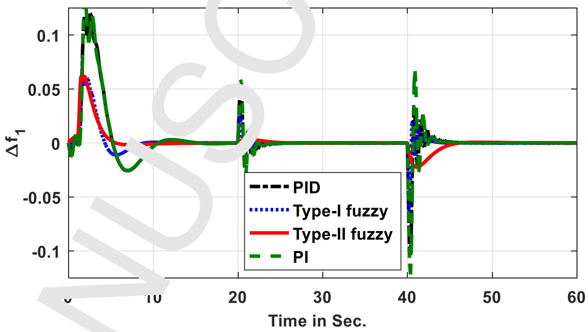

Fig. 9(b) Variation of area1 frequency due to ΔP_W

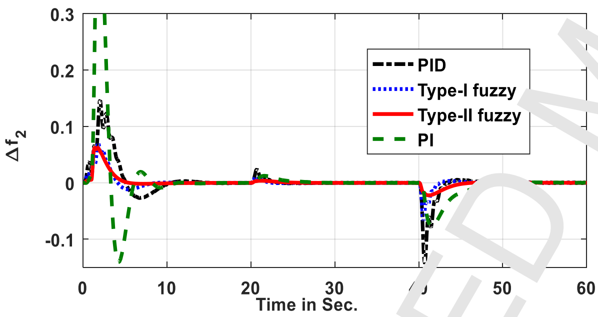

Fig. 9(c) Variation of area2 frequency due to ΔP_W

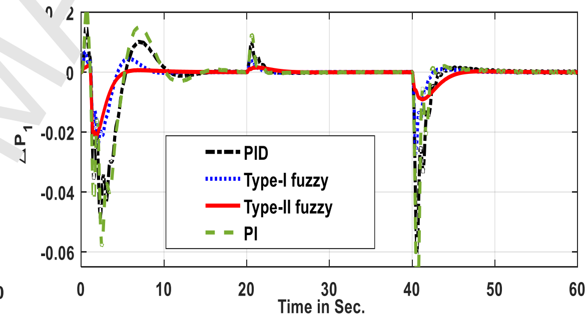

Fig. 9(d) Variation of tie-line power due to ΔP_W

Table.3 Performance indices of different responses due to I-SSO optimized controllers

Controller/ Performance	Type-II fuzzy PID Controller			Fuzzy PID Controller			PID Controller		
	Over shoot in Pu	Under shoot in Pu	Settling Time (Sec)	Over shoot in Pu	Under shoot in Pu	Settling Time (Sec)	Over shoot in Pu	Under shoot in Pu	Settling Time (Sec)
ΔF_1	0.06	-0.001	6.80	0.06	-0.01	7.92	0.12	-0.024	12.60
ΔF_2	0.062	---	6.20	0.07	-0.01	8.42	0.12	-0.03	11.22
ΔP_{12}	---	-0.020	6.42	0.002	-0.022	9.24	0.006	-0.042	10.82
ITAE	8.8312			22.0652			32.1088		

***Scenario-3*: Fluctuation in solar irradiation power only (ΔP_ϕ), , ΔP_L=0, ΔP_L=0**

For this study a solar irradiation power fluctuation signal shown in Fig.10(a) is effected at area1 at time t=0.5s. All deviated responses due to different optimized controllers are depicted in Fig.10. The deviation in frequency responses of area1 and area2 due to different optimized controllers are depicted in Fig.10(b-c) respectively and tie-line power deviation is shown in Fig.10(d). All the results conclude that, the responses are improved significantly with implementation of I-SSO optimized proposed type-II fuzzy controller.

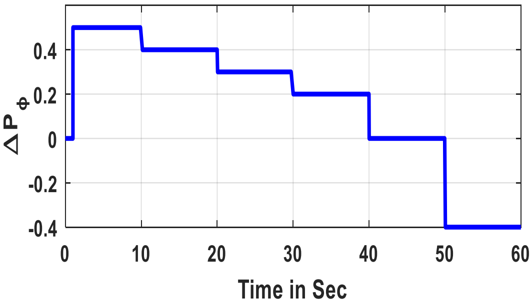

Fig. 10(a) Variation of solar irradiation power (ΔP_{Φ})

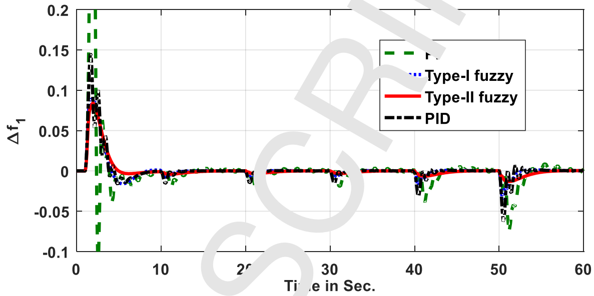

Fig. 10(b) Variation of area1 frequency due to ΔP_{Φ}

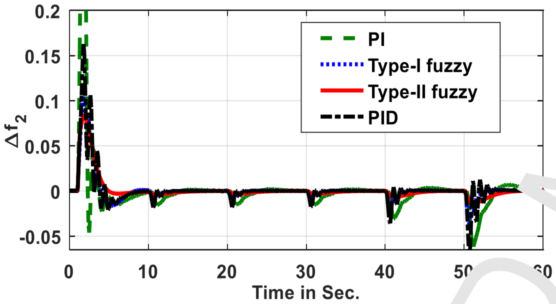

Fig. 10(c) Variation of area2 frequency due to ΔP_{Φ}

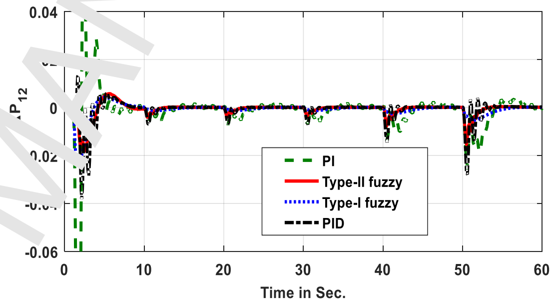

Fig. 10(d) Variation of tie-line power due to ΔP_{Φ}

***Scenario-4*: Effectiveness of all three uncertainties simultaneously ($\Delta P_L + \Delta P_{W} + \Delta P_{\Phi}$)**

The resultant response of three different uncertainties is shown in Fig.11(a) and is effected in area1 to obtain different dynamic responses for LFC study of MG system.

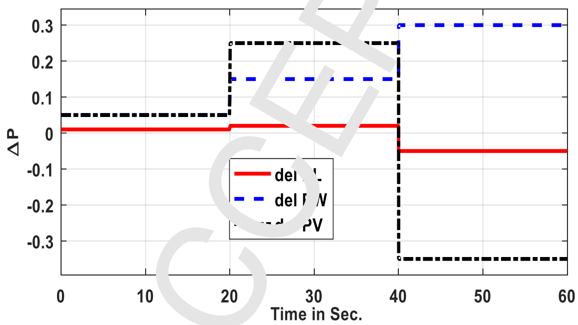

Fig. 11(a) Variation of three uncertainties ($\Delta P_L + \Delta P_{W} + \Delta P_{\Phi}$)

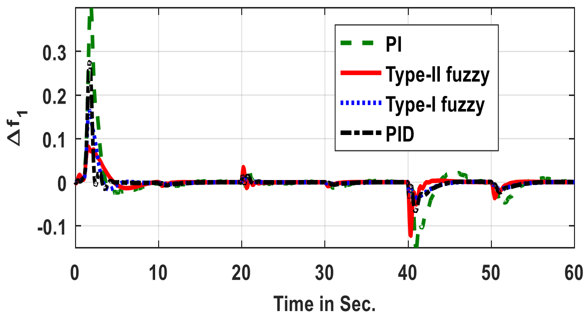

Fig. 11(b) Area1 frequency deviation

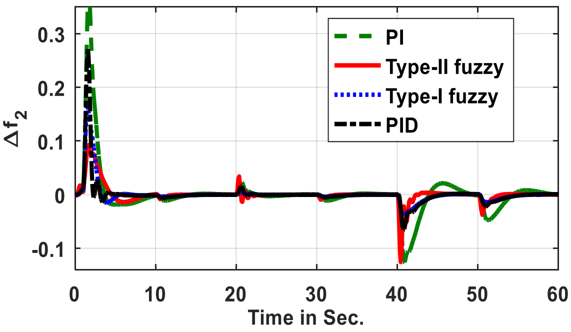

Fig. 11(c) Area2 frequency deviation.

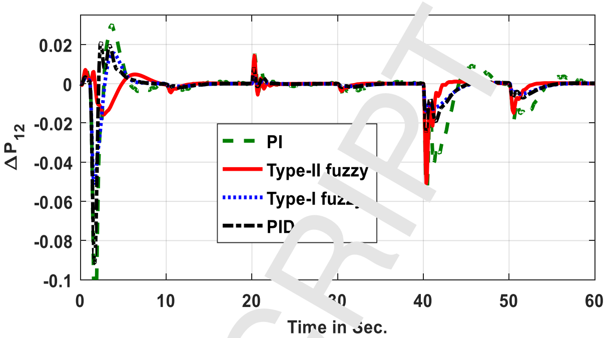

Fig. 11(d) Tie-line power deviation.

Dynamic responses obtained due to I-SSO tuned different controllers under the influence of all three uncertainties are depicted in Fig.11 which reflects supremacy of our proposed I-SSO tuned type-II fuzzy PID controller.

B. Technique Level

This section of the proposed study deals with to justify supremacy of proposed I-SSO technique over original SSO, PSO and GA algorithm under different uncertainties conditions of MG system. In regard to this the LFC study due to various uncertainties are demonstrated through different scenarios.

***Scenario-1*: Variation of only load (ΔP_L)**

In this case study to obtain LFC of an interconnected MG system a random pattern load (RLP) as shown in Fig.12(a) is effected in area1 at time t=0 while effected disturbances of wind and solar power is zero(ΔP_W=0, ΔP_ϕ=0). In regard to this disturbance, the deviated responses of frequency and tie-line power resulted due to different techniques optimized type-II fuzzy PID controller are depicted in this section. To obtain simulated dynamic responses, the optimal gain parameters of type-II fuzzy controller due to different techniques along with respective ITAE values are gathered in table.4.The deviation in frequency of area1 and area2 due to above uncertainty are depicted in Fig.12(b-c) respectively. The tie-line power deviation is given in Fig.12(d). Despite of their settling time, peak overshoot and peak undershoot, a significant improvement has been noticed in all dynamic responses resulted due to proposed I-SSO optimized type-II fuzzy PID controller. So our proposed approach exhibits more effectiveness over other implemented optimization techniques.

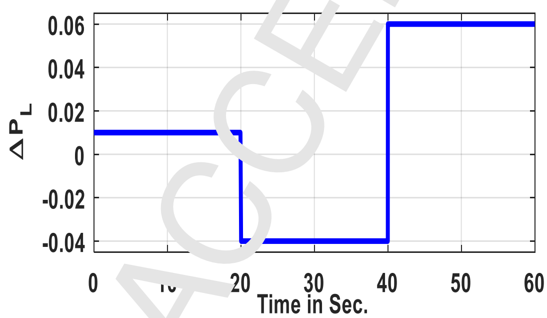

Fig. 12(a) Variation of load (Δ**P**$_L$)

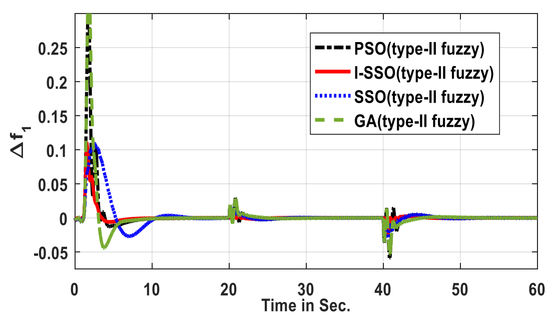

Fig. 12(b) Variation of area1 frequency due to Δ**P**$_L$

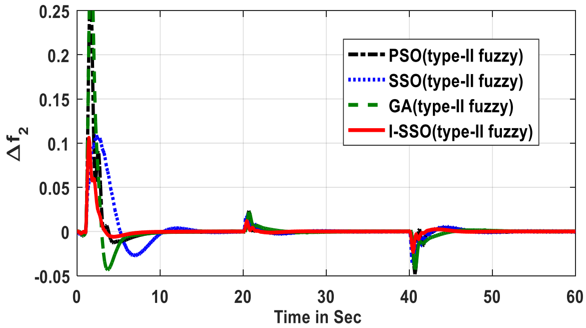

Fig. 12(c) Variation of area2 frequency due to Δ**P**$_L$

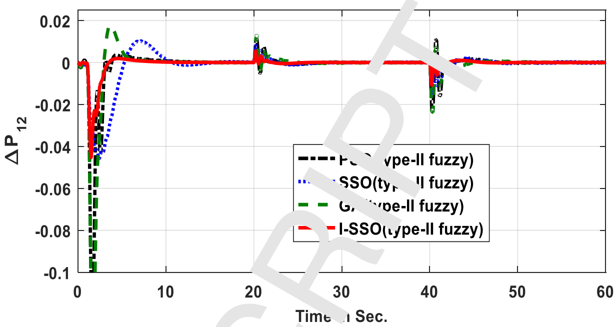

Fig. 12(d) Variation of tie-line power due to Δ**P**$_L$

Table.4 Optimal gain parameters of typa-II fuzzy controller due to different techniques with respective ITAE values

Area	Techniques	ITAE	Type-II fuzzy PID Controller				
			K_P	K_I	K_D	K_1	K_2
Area.1	GA	31.0158	-1.9988	-1.9696	-1.9902	0.9876	1.0212
	PSO	23.6332	-1.7978	-1.9[illegible]98	-1.9822	1.1012	-0.8018
	SSO	20.9682	-1.9706	-1.[illegible]568	-1.9814	-0.2918	1.4514
	I-SSO	8.8312	-1.9516	-0.969[illegible]	-1.9998	1.6024	-0.7654
Area.2	GA	31.0158	-1.6552	[illegible].9998	0.9028	1.5858	0.9896
	PSO	23.6332	-1.9992	-1.9[illegible]76	-1.9996	-0.9820	1.5698
	SSO	20.9682	-1.5138	[illegible]736	0.8416	1.4166	-0.6892
	I-SSO	8.8312	-0.8544	[illegible].9800	0.8706	0.9898	1.0212

***Scenario-2*: Fluctuation in wind power only (ΔP_W), ΔP_L=0, ΔP_ϕ=0**

For this study a wind power fluctuation signal shown in Fig.13 (a) is effected at area1 at time t=0. All deviated responses due to different optimization technique based type-II fuzzy PID controller are depicted in Fig.13.

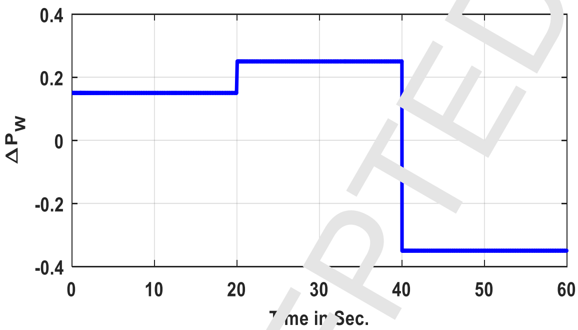

Fig. 13(a) Variation of wind power (Δ**P**$_W$)

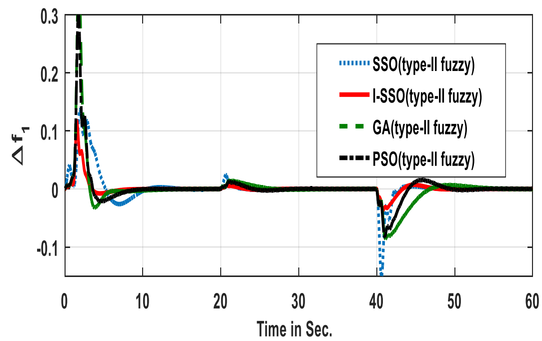

Fig. 13(b) Variation of area1 frequency due to Δ**P**$_W$

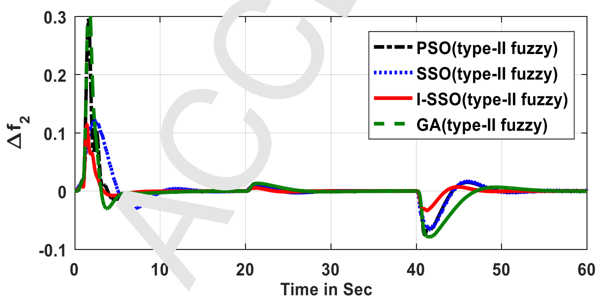

Fig. 13(c) Variation of area2 frequency due to Δ**P**$_W$

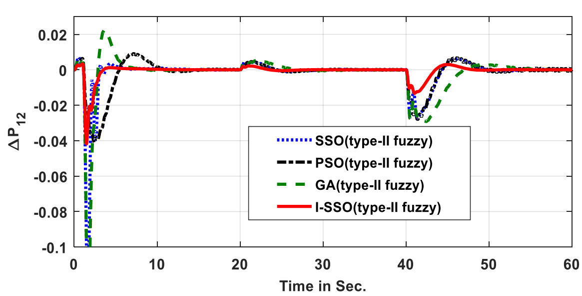

Fig. 13(d) Variation of tie-line power due to Δ**P**$_W$

Deviated frequency response of area1 and area2 area depicted in Fig.13(b-c) respectively where as tie-line power deviation is shown in Fig.13(d). It has been noticed through different dynamic responses that proposed I-SSO technique is more effectiveness over SSO, PSO and GA techniques in regard to LFC study of interconnected MG system.

***Scenario-3*: Fluctuation in solar irradiation power only (ΔP_{Φ}), , ΔP_L=0, ΔP_L=0.**

In this scenario a solar irradiation power fluctuation signal shown in Fig.14(a) is effected at area1 at time t=0.5s. The deviated in frequency responses of area1 and area2 due to different optimization technique based type-II fuzzy PID controller are depicted in Fig.14(b-c) respectively and the tie-line power deviation response is given through Fig.14(d). Critical analysis confers our proposed I-SSO algorithm exhibits superior performance over other implemented techniques in regard to settling time; peak overshoot and peak undershoot of all resulted dynamic responses

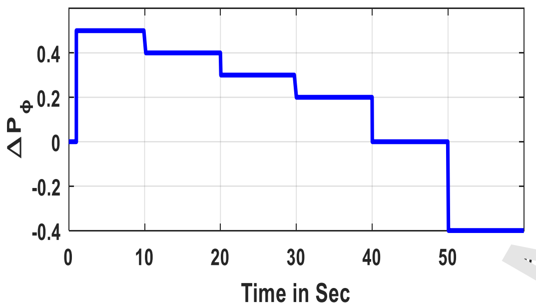

Fig. 14(a) Variation of solar irradiation power (ΔP_{Φ})

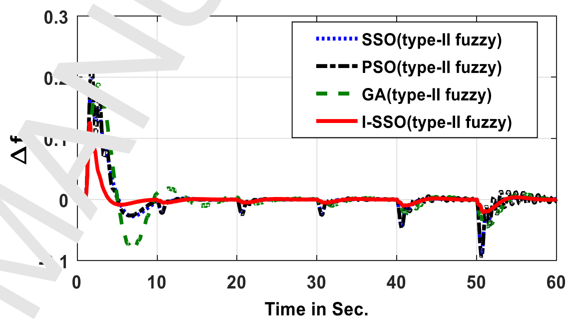

Fig. 14(b) Variation of area1 frequency due to ΔP_{Φ}

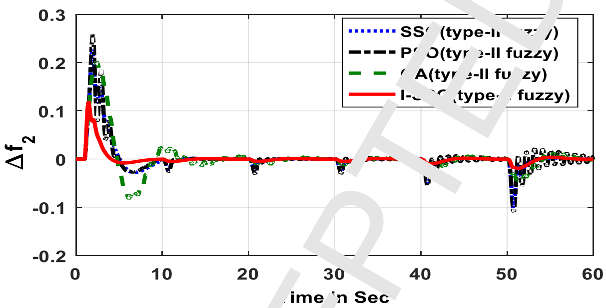

Fig. 14(c) Variation of area2 frequency due to ΔP_{Φ}

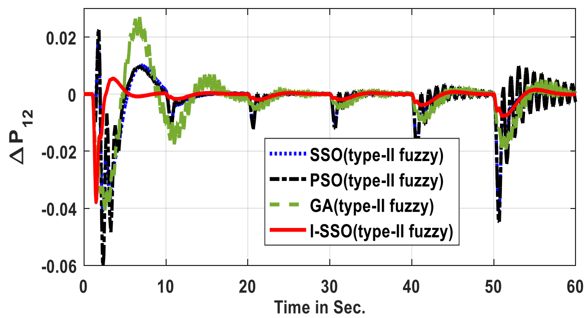

Fig. 14(d) Variation of tie-line power due to ΔP_{Φ}

***Scenario-4*: Effectiveness of all three uncertainties simultaneously ($\Delta P_L + \Delta P_W + \Delta P_{\Phi}$)**

The response of three different uncertainties effected simultaneously is given in Fig.11 (a) and is effected in area1 to obtain different dynamic responses for LFC study of MG system. Deviation in both area frequency responses due to different technique based type-II fuzzy controller are depicted in Fig.15 (a-b) respectively where as tie-line power deviation response is depicted in Fig.15(c).

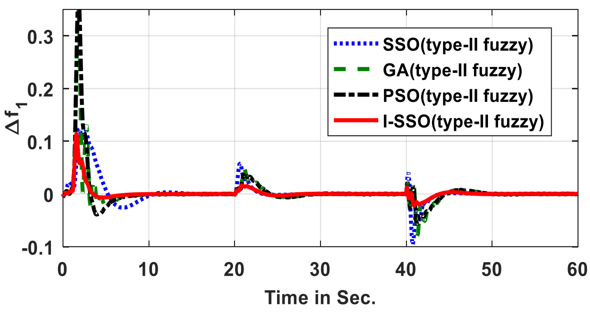

Fig. 15(a) Area1 frequency deviation.

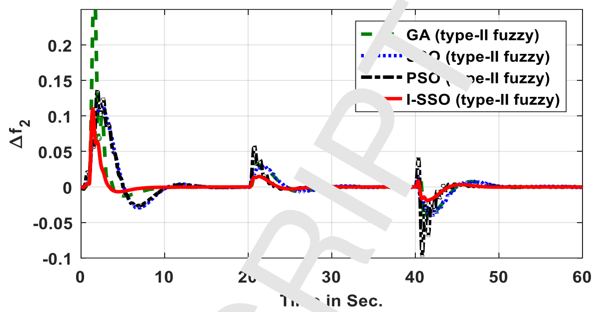

Fig. 15(b) Area2 frequency deviation.

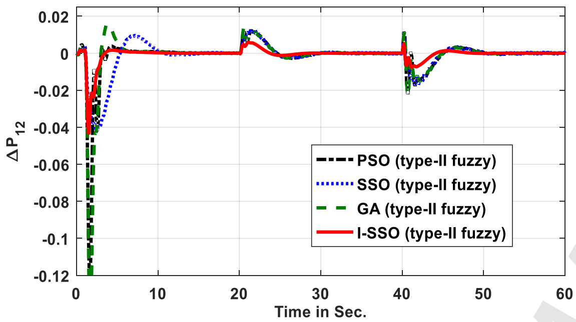

Fig. 15(c) Tie-line power frequency deviation.

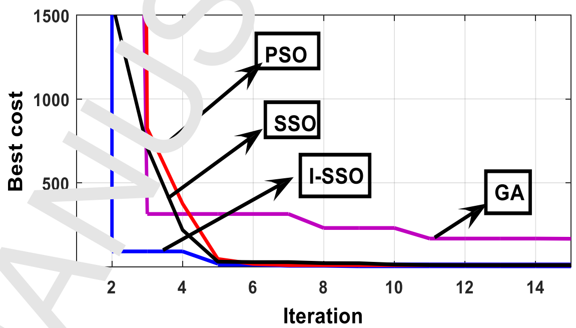

Fig. 15(d) Convergence Curve.

The dynamic responses has been depicted through different conditions reveal that proposed I-SSO optimized type-II fuzzy PID controller exhibits more effectiveness over other techniques based proposed type-II fuzzy controller. The convergence curve shown in Fig.15(d) reveals faster convergence of proposed I-SSO algorithm and resulted nominal values gathered in table.3 concludes that responses obtained due to I-SSO optimized type-II fuzzy PID controller exhibits least settling time, minimal peak overshoot and undershoot. Overall critical discussions on section-A and section-B reveal that proposed I-SSO optimized type-II fuzzy PID controller exhibits superior performance in regard to LFC study of an islanded multi-area interconnected MG system.

6. Conclusion

The article has focused to propose a robust type-II fuzzy PID controller for load frequency control in an isolated two-area interconnected microgrid (MG) system under various uncertainties. The different uncertainties (ΔP_L, ΔP_W and ΔP_ϕ) are effected individually and finally combined to develop different dynamic responses (Δf and ΔP_{tie}) in presence of proposed type-II fuzzy PID controller. To obtain optimal gain values of above proposed controller, a meta-heuristic improved salp swarm optimization (I-SSO) algorithm has been implemented and it has seen that the proposed type-II fuzzy PID controller is more effective over other implemented controllers like type-I fuzzy controller, PID and PI controllers. The time domain dynamic responses reveal that, proposed type-II fuzzy PID controller is able to balance the power generation and demand properly and control both system frequency and tie-line power effectively. In technique level, the performance of proposed I-SSO algorithm is compared with original

SSO, PSO and GA algorithm through different dynamic responses and numerical results which confers supremacy of proposed I-SSO algorithm under different uncertainties conditions for LFC of interconnected MG system. Finally it has been suggested that proposed I-SSO optimized type-II fuzzy PID controller exhibits tremendous performances over other implemented approaches for LFC analysis of an islanded two area interconnected microgrid system.

7. Appendix

D_i = damping coefficient i^{th} area = 0,012 (pu/Hz); M_i = Inertia constant of i^{th} area = 0.2 (pu/s); i= 1,2; T_{FC} = FuelCell time constant = 4s; T_{BES} = Battary energy time constant = 0.1s; T_{FES} = Flywheel energy storage time constant =0.1s; T_{DEG} = Diesel engine generator time constant = 2s; T_{MT} = Microturbine time constant = 2s; T_{WTG} = Wind turbine generator time constant = 1.5s; T_{PV} = Photo Voltaic cell time constant = 1.8s; B = Frequency biasing factor = 0.425 pu MW /Hz. ; R = Regulation =0.05 Hz/Mw; T_{12} = Time coefficient=1.6 s.

Reference

1. D. E. Olivares, A. Mehrizi-Sani, A. H. Etemadi, C. A. Cañizares, R. Iravani, M. Kazerani , G. A. Jimenez-Estevez, Trends in microgrid control, IEEE Transactions on smart grid. *5*(4) (2014) 1905-1919.
2. M. J. Davison, T. J. Summers, C. D. Townsend, A review of the distributed generation landscape, key limitations of traditional microgrid concept & possible solution using an enhanced microgrid architecture. In Power Electronics Conference (SPEC), 2017 IEEE Southern (pp. 1-6). IEEE.
3. L. Wang, L. Zhang, C. Xu, A. T. Eseye, J. Zhang, D. Zheng, Dynamic Economic Scheduling Strategy for a Stand-alone Microgrid System Containing Wind, PV Solar, Diesel Generator, Fuel Cell and Energy Storage:-A Case Study. In IOP Conference Series: Earth and Environmental Science (Vol. 168, No. 1, p. 012006) (2018). IOP Publishing.
4. K. V. Vidyanandan, N. Senroy, Frequency regulation in a wind–diesel powered microgrid using flywheels and fuel cells, IET Generation, Transmission & Distribution. 10(3) (2016) 780-788.
5. M. E. Lotfy, T. Senjyu , M. A. F. Farahat, A. F. Abdel-Gawad, A. Yona, A frequency control approach for hybrid power system using multi-objective optimization, Energies. *10*(1) (2017) 80.
6. J. Qiu , J. Zhao , H. Yang , D. Wang , Z. Y. Dong, Planning of solar photovoltaics, battery energy storage system and gas micro turbine for coupled micro energy grids, Applied Energy. 219 (2018)361-369.
7. M. Faisal, M. A. Hannan, P. J. Ker, A. Hussain, M. Mansur, F. Blaabjerg, Review of energy storage system technologies in microgrid applications: Issues and challenges. IEEE Access. (2018).
8. S. A. Hamidi, D. M. Ionel, A. Nasiri, Batteries and Ultracapacitors for Electric Power Systems with Renewable Energy Sources. Renewable Energy Devices and Systems with Simulations in MATLAB® and ANSYS®.(2017).
9. O. Palizban, K. Kauhaniemi, Hierarchical control structure in microgrids with distributed generation: Island and grid-connected mode, Renewable and Sustainable Energy Reviews. *44* (2015) 797-813.
10. J. Li, Y. Liu, L. Wu, Optimal Operation for Community-Based Multi-Party Microgrid in Grid-Connected and Islanded Modes, IEEE Transactions on Smart Grid. *9*(2) (2018)756-765.
11. X. Qi , Y. Bai , H. Luo , Y. Zhang , G. Zhou, Z. Wei, Fully-distributed Load Frequency Control Strategy in an Islanded Microgrid Considering Plug-In Electric Vehicles, Energies, *11*(6) (2018)1613.
12. Y. Xu, H. Sun, W. Gu, Y. Xu , Z. Li , Optimal Distributed Control for Secondary Frequency and Voltage Regulation in an Islanded Microgrid, IEEE Transactions on Industrial Informatics.(2018).
13. M. H. Khooban, T. Niknam, F. Blaabjerg, P. Davari, T. Dragicevic, A robust adaptive load frequency control for micro-grids, ISA transactions. *65* (2016) 220-229.
14. M. R. Khalghani, M. H. Khooban, E. Mahboubi-Moghaddam, N. Vafamand, M. Goodarzi, A self-tuning

load frequency control strategy for microgrids: Human brain emotional learning, International Journal of Electrical Power & Energy Systems. *75*(2016) 311-319.

15. M. Sato, K. Ohara, K. Ono, Y. Mori, K. Osato, T. Okabe, H. Muraoka, Development of Micro Grid Kalina Cycle® System–The First Demonstration Plant in Hot Spring Area in Japan, Development. *19* (2015) 25.
16. A. M. A. Acuzar, I. P. E. Arguelles, J. C. S. Elisan, J. K. D. Gobenciong, A. M. Soriano, J. M. B. Rocamora, Effects of weather and climate on renewable energy resources in a distributed generation system simulated in Visayas, Philippines, In Humanoid, Nanotechnology, Information Technology, Communication and Control, Environment and Management (HNICEM), 2017 IEEE 9th International Conference on (pp. 1-6). IEEE.
17. K. Li, K. J. Tseng, Energy efficiency of lithium-ion battery used as energy storage devices in micro-grid, In Industrial Electronics Society, IECON 2015-41st Annual Conference of the IEEE (pp. 005235-005240). IEEE.
18. C. Wei, Z. M. Fadlullah, N. Kato, I. Stojmenovic, On optimally reducing power loss in micro-grids with power storage devices. IEEE Journal on Selected Areas in Communications, *32*(7) (2014) 1361-1370.
19. S. Marzal, R. Salas-Puente, R. González-Medina, E. Figueres, G. Garcerá, Peer-to-peer decentralized control structure for real time monitoring and control of microgrids. IEEE 26th International Symposium on Industrial Electronics (ISIE) (pp. 140-145). (2017),IEEE.
20. L. Y. Lu, C. C. Chu, Consensus-based secondary frequency and voltage droop control of virtual synchronous generators for isolated AC micro-grids. IEEE Journal on Emerging and Selected Topics in Circuits and Systems. *5*(3) (2015) 443-455.
21. A. H. Etemadi,E. J Davison, R. Iravani, A decentralized robust control strategy for multi-DER microgrids—Part I: Fundamental concepts, IEEE Transactions on Power Delivery. *27*(4) (2012). 1843-1853.
22. H. Bevrani, M. R. Feizi, S. Ataee, Robust Frequency Control in an Islanded Microgrid: ${H} _ {\infty} $ and $\mu $-Synthesis Approaches, IEEE transactions on smart grid. *7*(2) (2016) 706-717.
23. A. Kahrobaeian, Y. A. R. I. Mohamed, Direct Single-Loop/spl mu/-Synthesis Voltage Control for Suppression of Multiple Resonances in Microgrids with Power-Factor Correction Capacitors, IEEE Transactions on Smart Grid. *4*(2) (2013)1150-1161.
24. R. K. Khadanga, S. Padhy, S. Panda, A. Kumar, Design and analysis of multi-stage PID controller for frequency control in an islanded micro-grid using a novel hybrid whale optimization-pattern search algorithm. International Journal of Numerical Modelling: Electronic Networks, Devices and Fields. e2349(2018).
25. N. L. Diaz, T. Dragicevic, J. C. Vasquez, J. M. Guerrero, Fuzzy-logic-based gain-scheduling control for state-of-charge balance of distributed energy storage systems for DC microgrids. In Applied Power Electronics Conference and Exposition (APEC), 2014 Annual IEEE (pp. 16-20).
26. R. K. Khadanga, S. Padhy, S. Panda, A. Kumar, Design and Analysis of Tilt Integral Derivative Controller for Frequency Control in an Islanded Microgrid: A Novel Hybrid Dragonfly and Pattern Search Algorithm Approach. Arabian Journal for Science and Engineering. *43*(6) (2018)3103-3114.
27. R. Sepulveda, P. Melin, A. R. Díaz, A. Mancilla, O. Montiel, Analyzing the effects of the footprint of uncertainty in type-2 fuzzy logic controllers. Engineering Letters, *13*(2) (2006)138-147.
28. E. Ontiveros, P. Melin , O. Castillo, Impact Study of the Footprint of Uncertainty in Control Applications Based on Interval Type-2 Fuzzy Logic Controllers. In Fuzzy Logic Augmentation of Neural and Optimization Algorithms: Theoretical Aspects and Real Applications, Springer, Cham. (2018) 181-197.
29. H. Hellendoorn, C.Thomas, Defuzzification in fuzzy controllers, Journal of Intelligent & Fuzzy Systems. *1*(2) (1993). 109-123.
30. N. Patnana, S. Pattnaik, V. P. Singh, Salp Swarm Optimization Based PID Controller Tuning for Doha Reverse Osmosis Desalination Plant.

31. S. Mirjalili, A. H. Gandomi, S. Z. Mirjalili, S. Saremi, H. Faris, S. M. Mirjalili, Salp Swarm Algorithm: A bio-inspired optimizer for engineering design problems, Advances in Engineering Software. *114*(2017) 163-191.
32. M.Köppen, R. Vicente-Garcia, B. Nickolay, Fuzzy-pareto-dominance and its application in evolutionary multi-objective optimization.In International Conference on Evolutionary Multi-Criterion Optimization. Springer, Berlin, Heidelberg. (2005) 399-412.
33. T. Wagner, N. Beume, B. Naujoks, Pareto-, aggregation-, and indicator-based methods in many-objective optimization. In International conference on evolutionary multi-criterion optimization Springer, Berlin, Heidelberg. (2007) 742-756.